ISSN (Print) 1226-1750
ISSN (Online) 2233-6656
Journal of Magnetics 26(3), 239-242 (2021) https://doi.org/10.4283/JMAG.2021.26.3.239

Thermally Excited Spin Waves of NiFe Nano-ring Arrays on Anodic Aluminum Oxide Templates

Seungha Yoon*, Deayun Lim, and Taewon Ha

Green Energy & Nano Technology R&D Group, Korea Institute of Industrial Technology (KITECH), 6, Chemdangwagi-ro 208-gil, Buk-gu, Gwangju, Republic of Korea

(Received 28 July 2021, Received in final form 8 September 2021, Accepted 9 September 2021)

The patterned substrates have been widely developed for various applications in the nanotechnology. In particular, the magnetic ring arrays could be utilized to not only the magnetic devices, such as memories and logics, but also magnetic stealth films using spin wave excitations. In this works, the magnetic switching behaviors and the thermally excited spin wave properties of the NiFe (permalloy) ring arrays on the anodic aluminum oxide template with carbon nanotubes were investigated. With increasing the diameter of the rings, the larger dipole interactions induced the larger coercive field of the array films in the plane directions. At the magnetically saturation conditions, the smaller diameter of the rings produced the single and broad spin wave absorptions due to the isotropic magnetic domains in both the horizontal and the vertical directions. When the size of the ring increased, each component felt different magnetic anisotropy field so that the two spin wave excitation peaks revealed. In terms of the mass production of the magnetic nano-ring arrays on the anodic aluminum oxide template, the various size and the shapes of the magnetic ring patterns could be good candidates for the rf stealth films of the defense industries.

Keywords : magnetic ring, array, AAO

1. Introduction

The sub-micrometer magnetic patterns with various shapes have been widely studied for the future applications, such as magnetic memories, logic devices and functional plates. In particular, the ring shape with sub-micrometer sizes has been widely investigated due to the complex several intermediate states during the magnetization switching depending on the ring size and the materials [1-4]. Recently the template-assisted fabrication methods using carbon nanotube (CNT) stamps on the anodic aluminum oxide (AAO) substrate for the sub-micrometer ring arrays were reported [5-7]. Comparing to the e-beam lithography techniques, this template-assisted fabrications is cheaper and faster with the mass production. Those patterns could be utilized to transfer the ring patterns to another substrate without further lithography process. Therefore, it is very promised techniques for the industrial applications.

Another possible application of widely well-ordered ring patterns might be a stealth materials for defense vehicles or aero flights. The Radar-absorbing materials are well-known as the polymer-based materials with specially designed and shaped for particular radio frequency ranges. However, there are also many efforts to increase the functionality and the efficiency of the stealth films using magnetic materials with the various patterns.

In this study, the diameter of the CNT ring stamps on the AAO templates are utilized to fabricate the NiFe ring arrays with a constant density of ~1×10^{10} cm^2. The basic magnetic properties and the spin waves excitation from absorbing the radio frequency signals of the NiFe ring arrays were investigated and suggested to utilize a stealth materials for defense industry [8-10].

2. Experiment

The fabrication process of the NiFe ring arrays was started from the preparation of the sub-micrometer ring array template. The AAO substrate was utilized to vertically grow CNT sub-micrometer ring patterns. The amorphous carbon on the surface of the stamps was

*Corresponding author: Tel: +82-62-600-6580
Fax: +82-62-600-6109, e-mail: yoonsh@kitech.re.kr

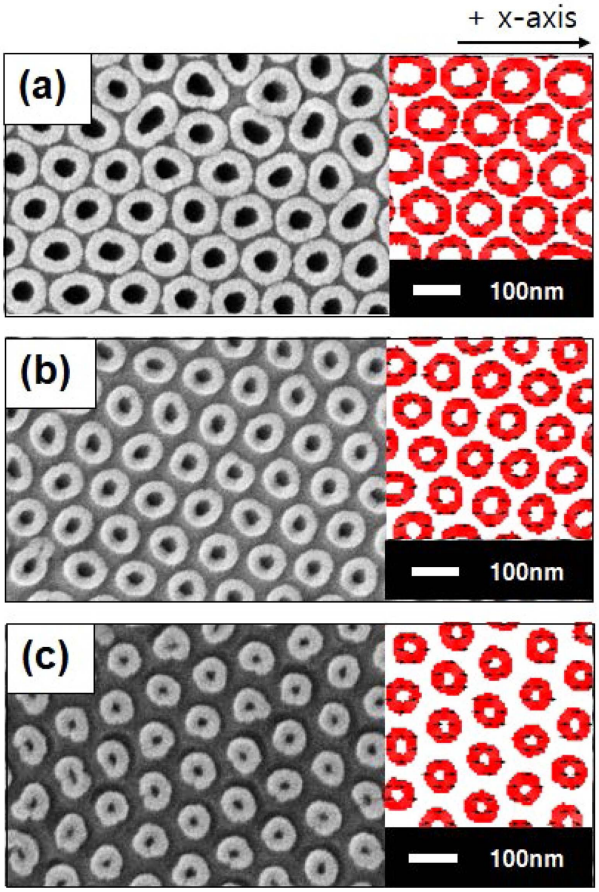

Fig. 1. The SEM images of the magnetic ring arrays, when the diameter of the ring varied from (a) 100 nm, (b) 90 nm, and (c) 70 nm.

removed using an Ar ion milling process and a wet-etching process. Then Ta (3 nm)/NiFe (10 nm)/Ta(3 nm) layers were deposited on top of the CNTs on the AAO templates with the size of 0.5×1 cm^2 with the growth rate of 0.01 nm/sec using ultra high vacuum magnetron sputter, which has the base pressure of ~0.5×10^{-10} Torr. The NiFe ring arrays on the CNT stamps were confirmed using the scanning electron microscope (SEM). Because of a constant density of the patterns, the gap between the ring patterns increased with deceasing the diameter of the NiFe ring. The NiFe ring arrays with the diameter 100 nm, 90 nm, and 70 nm are shown in Fig. 1(a), (b), and (c), respectively.

The magnetization curves of the NiFe ring arrays on the CNT stamps were measured by a vibrating sample magnetometer (VSM) at room temperature. In order to verify the magnetic interaction between the NiFe rings, we performed the OOMMF simulation with the real patterns based on the SEM images, as shown as the red rings in the insets of Fig. 1. The thermally excited spin waves depending on the radio frequency were investigated using micro-Brillouin light scattering (BLS) spectroscopy with the spot diameter of approximately 250 nm using a high magnification of microscope objective (100×). The 1 mW incident beam is generated by a 532 nm wavelength diode-pumped solid laser (DPSS) and focused on the NiFe ring arrays. The reflected light from the NiFe ring surfaces passes through a (3 + 3)-pass tandem Fabry Perot interferometer to produce the frequency domain spectrum.

3. Results and Discussion

The magnetization reversal of NiFe sub-micrometer ring arrays is investigated when an external magnetic field varied from -15 mT to 15 mT in the sample plane x-direction. The OOMMP simulation was performed with the real ring array patterns with 1 nm volume unit cells. Because of the thermal effect on the VSM measurement in the room temperature, as shown in the Fig. 2, the switching behaviors were different to the simulation

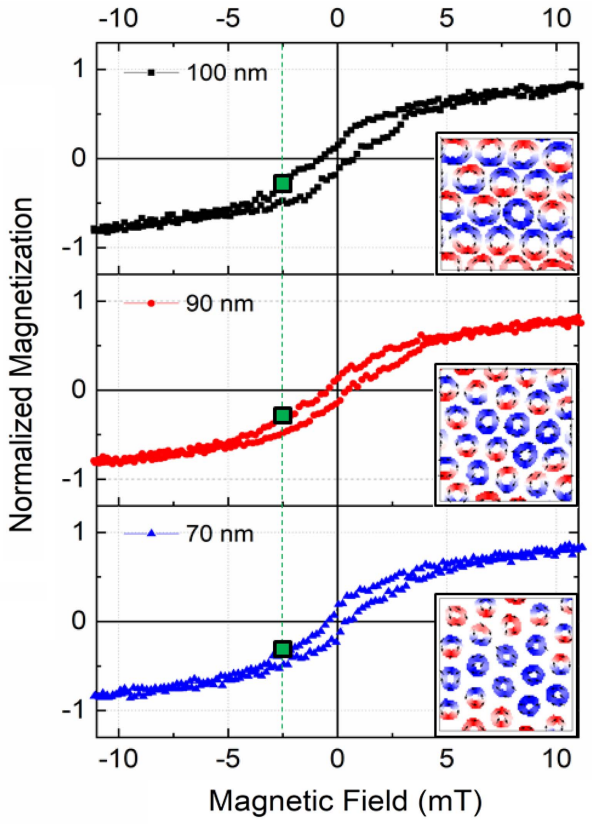

Fig. 2. The magnetization switching behaviors of the magnetic nano-ring arrays of diameter 100 nm, square, 90 nm, and 70 nm are represented by plots of black- square, red-circle, and blue-triangle, respectively. The insets shows the magnetic switching of the nano-rings at the -2.5 mT from the positively saturation in the x-axis.

results. However, the magnetic dipole interaction between the rings were clearly shown in the magnetization curves depending on an external magnetic field in the x-axis. The gap average between the nano-rings of diameter 100 nm was less than 10 nm. In this distance, the magnetic domain in the nano-ring could be coupled with another domain in the others. However, when the diameter of the ring decreased, the larger gap made the magnetic switching of the nano-rings more decoupled. The weaker dipole interactions between the rings were confirmed from the simulation results, as shown in the insets of Fig. 2, at the magnetic field -2.5 mT (the green squares) after the magnetic rings were positively saturated in the x-axis.

In order to confirm the spin wave excitation in the radio frequency ranges, thermal excited spin waves were measured using micro BLS system at room temperature. Because the spot size of the focused beam on the sample surface is approximately 200 nm, we have assumed that the spin wave excitation signals were collected from about 3

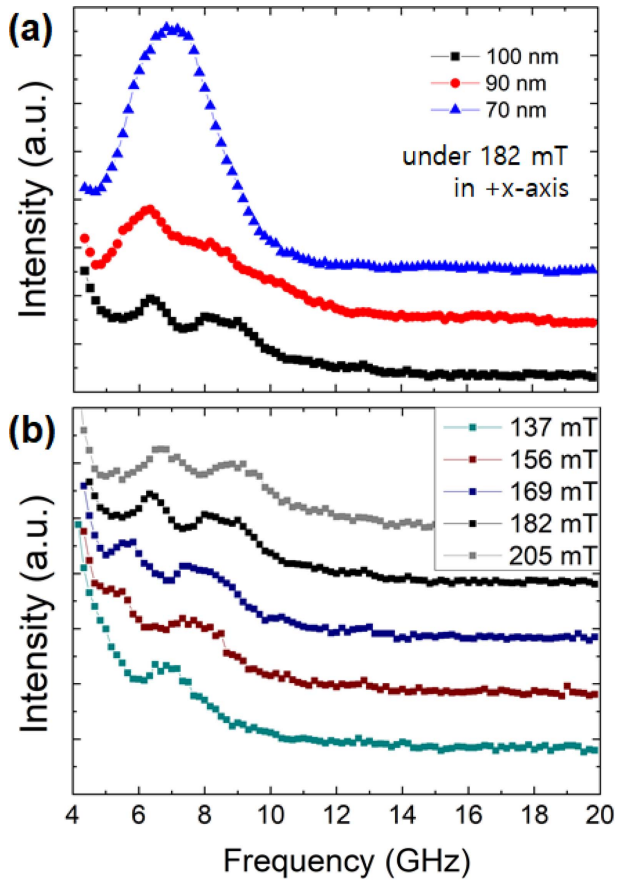

Fig. 3. (a) Brillouin light scattering intensity of the magnetic nano-ring arrays depending on the frequency. (b) Two peaks from the magnetic ring of diameter 100 nm have been shfited toward the higher magnetic frequencies with increainsg the applied magnetic field in the horizontal film plane direction.

magnetic rings independent on its diameter due to the same density of the magnetic rings on the unit area. The micro-BLS measurement only shows the spin wave excitations in the plane directions of the NiFe ring arrays. There were two main BLS peaks (around 6.3 GHz and 9 GHz) related to the horizontal and the vertical components at the saturation condition in the ring arrays of diameter 100 nm. In terms of the magnetization saturation condition in the horizontal direction, it could be thought that the different anisotropy field of the horizontal and the vertical component could arise the different peaks on the frequency sweep of the BLS measurement. On the other hand, the single and broad peak at around 7 GHz was observed, because of the similar anisotropy condition between the horizontal and the vertical components in the magnetic ring arrays of diameter 70 nm. The micro-BLS results depending on the magnetic ring size in the arrays were shown in Fig. 3(a) with the uniformly shifted offset in order to clearly show the peaks better, when the magnetic field of 182mT was applied in the plane x-direction. To confirm that those peaks were related to the magnetic spin wave excitation from the magnetic ring arrays, we applied the magnetic field from 137 mT to 205 mT on the magnetic ring array of the diameter 100 nm. As shown in the Fig. 3(b), the two peaks were linearly shifted with increasing the magnetic field in the film plane x-direction due to the dispersion relation of the spin waves.

4. Conclusion

The magnetization switching behaviors and the spin wave excitation properties of the NiFe magnetic rings on the CNT stamps of AAO template were measured. The dipole coupling between the magnetic rings were significant when the rings located closely. When the NiFe rings were sufficiently saturated from the magnetic field in the plan x-direction, the horizontal and vertical spin wave components were observed from the large diameter rings. While the diameter of the magnetic rings decreased, the dipole interaction also decreased during the magnetization switching behaviors. In addition, the spin waves from the horizontal and vertical components were mixed so that the single BLS peak was observed. Because the spin wave excitation frequency of the NiFe rings was simply controlled by varying the magnetic field, the magnetic ring arrays could be utilized to the stealth materials in the defense industry. Therefore, the large output of the magnetic pattern arrays depending on the size, the shape and the material of the unit element provides various rf observation frequencies for the stealth function.

Acknowledgement

This work is supported by Korea Institute of Industrial Technology (KITECH).

References

[1] C. A. Ross, M. Hwang, M. Shima, J. Y. Cheng, M. Farhoud, T. A. Savas, H. I. Smith, W. Schwarzacher, F. M. Ross, M. Redjdal, and F. B. Humphrey, Phys. Rev. B **65**, 144417 (2002).

[2] Seungha Yoon, Youngman Jang, Chunghee Nam, J.A. Currivan, B. K. Cho, and C. A. Ross, IEEE Magn. Lett. **3**, 4000104 (2012).

[3] S. Yoon, S. Ho Lee, W. Kwak, C. Nam, W. Bae Kim, and B. K. Cho, Journal of Applied Physics **115**, 17B511 (2014).

[4] C. Nam, M. D. Mascaro, and C. A. Ross, Appl. Phys. Lett. **97**, 012505 (2010).

[5] S. H. Lee, S. Yoon, H. Jeong, M. Han, S. M. Choi, J. G. Kim, J.-W. Park, G. Y. Jung, B. K. Cho, and W. B. Kim, Nanoscale **5**, 10653 (2013).

[6] S. H. Lee, B. Cho, S. Yoon, H. Jeong, S. Jon, G. Y. Jung, B. K. Cho, T. Lee, and W. B. Kim, ACS Nano **5**, 5543 (2011).

[7] Y.-S. Kim, H.-J. Ahn, S. H. Nam, S. H. Lee, H.-S. Shim, and W. B. Kim, J. Nanosci. Nanotechnol. **8**, 4803 (2008).

[8] F. Bigourdan, R. Pierrat, and R. Carminati, Opt. Express **27**, 8666 (2019).

[9] C. Wang, M. Chen, H. Lei, K. Yao, H. Li, W. Wen, and D. Fang, Composites Part B: Engineering **123**, 19 (2017).

[10] H.-K. Jang, W.-H. Choi, C.-G. Kim, J.-B. Kim, and D.-W. Lim, Composites Part B: Engineering **56**, 178 (2014).